



**HAL**  
open science

## **Inhibition of the replication of SARS-CoV-2 in human cells by the FDA-approved drug chlorpromazine**

Marion Plaze, David Attali, Matthieu Prot, Anne-Cécile Petit, Michael Blatzer, Fabien Vinckier, Laurine Levillayer, Jeanne Chiaravalli, Florent Perin-Dureau, Arnaud Cachia, et al.

### ► To cite this version:

Marion Plaze, David Attali, Matthieu Prot, Anne-Cécile Petit, Michael Blatzer, et al.. Inhibition of the replication of SARS-CoV-2 in human cells by the FDA-approved drug chlorpromazine. International Journal of Antimicrobial Agents, 2021, 57 (3), pp.106274. 10.1016/j.ijantimicag.2020.106274 . pasteur-03277133

**HAL Id: pasteur-03277133**

**<https://pasteur.hal.science/pasteur-03277133>**

Submitted on 15 Mar 2023

**HAL** is a multi-disciplinary open access archive for the deposit and dissemination of scientific research documents, whether they are published or not. The documents may come from teaching and research institutions in France or abroad, or from public or private research centers.

L'archive ouverte pluridisciplinaire **HAL**, est destinée au dépôt et à la diffusion de documents scientifiques de niveau recherche, publiés ou non, émanant des établissements d'enseignement et de recherche français ou étrangers, des laboratoires publics ou privés.



Distributed under a Creative Commons Attribution - NonCommercial 4.0 International License



29 **Abstract** (249 words)

30 **Introduction:** Urgent action is needed to fight the ongoing COVID-19 pandemic by reducing the number of  
31 infected people along with the infection contagiousness and severity. Chlorpromazine (CPZ), the prototype of  
32 typical antipsychotics from the phenothiazine group, is known to inhibit clathrin-mediated endocytosis and  
33 acts as an antiviral, in particular against SARS-CoV-1 and MERS-CoV. The aim of this *in vitro* study was to test  
34 CPZ against a SARS-CoV-2 isolate in monkey and human cells.

35 **Material and methods:** Monkey VeroE6 cells and human alveolar basal epithelial A549-ACE2 cells were  
36 infected with SARS-CoV-2 in presence of different concentrations of CPZ. Supernatants were harvested at day  
37 2 and analysed by RT-qPCR for the presence of SARS-CoV-2 RNA. Cell viability was assessed on non-infected  
38 cells.

39 **Results:** We evidenced an antiviral activity of CPZ against SARS-CoV-2 in monkey VeroE6 cells with an IC50 of  
40 8.2  $\mu\text{M}$ , a CC50 of 13.5 $\mu\text{M}$  and a SI of 1.65. In human A549-ACE2 cells, CPZ was also associated with an anti-  
41 SARS-CoV-2 activity, with an IC50 of 11.3  $\mu\text{M}$ , a CC50 of 23.1  $\mu\text{M}$  and a SI of 2.04.

42 **Discussion:** Even though the measured SI are low, such IC50 measured *in vitro* may translate to CPZ dosage  
43 used in clinical routine because of CPZ high biodistribution in lungs and in saliva. Also, CPZ brain distribution  
44 could be of high interest for treating or preventing the neurological and psychiatric forms of COVID-19.

45 **Conclusions:** These preclinical findings support clinical investigation of the repurposing of CPZ, a largely used  
46 drug with mild side effects, in COVID-19 treatment.

47

48 **Keywords:** chlorpromazine; SARS-CoV-2; COVID-19; repurposing of molecules; human cells

49

50 **Chemical compounds studied in this article** Chlorpromazine (PubChem CID: 2726)

51

52

53 **Introduction**

54 From the beginning of the COVID-19 outbreak we observed in Sainte Anne hospital (GHU PARIS Psychiatrie &  
55 Neurosciences, Paris, France) a higher prevalence of symptomatic and severe forms of COVID-19 infections  
56 among health care professionals (~14%) compared to patients in psychiatric wards (~4%) [1]. This unexpected  
57 finding, that patients with more comorbidities and risk factors (overweight, cardiovascular disorders, etc.)  
58 seem to be protected against symptomatic and severe forms of COVID-19, drew our interest to decipher  
59 putative factors that could mediate this anti-SARS-CoV-2 protection. Because patients in psychiatric wards  
60 receive psychotropic medications, we screened the literature for antiviral effects associated with those drugs.  
61 This literature analysis identified chlorpromazine (CPZ), the prototype of phenothiazine-type antipsychotics, as  
62 the lead candidate [1]. The reasons why CPZ was identified as the lead candidate among psychotropic drugs  
63 are multiple. Firstly, in addition to its antipsychotic activity, CPZ has been used for decades in virology. On the  
64 one hand, *in vitro* studies have demonstrated CPZ antiviral properties, for example against influenza [2],  
65 hepatitis viruses [3], alphaviruses [4], JC virus [5], Japanese encephalitis virus [6], bronchitis-virus [7], MHV-2  
66 [8], Zika virus [9] or dengue virus [10]. On the other hand, CPZ is the leading drug inhibiting clathrin-mediated  
67 endocytosis [11–14] – via translocation of clathrin and AP2 from the cell surface to intracellular endosomes  
68 [12] – and therefore is commonly used to determine the pathways of entry of viruses into cells [11–14]. In a  
69 recent review article, the authors underlined the therapeutic potential of targeting clathrin-mediated  
70 endocytosis – essential for coronavirus cell entry [15] – to tackle SARS-CoV-2 [16].  
71 Secondly, CPZ has been shown to have antiviral activity against coronaviruses in multiple studies [17–20]. It  
72 was identified active against both MERS-CoV and SARS-CoV-1 in a screen of 348 FDA-approved drugs, together  
73 with three other compounds (chloroquine, loperamide, lopinavir), using different cell lines [17]. Similar results  
74 were obtained in a different library screen [18], as well as in another study using primary human monocytes  
75 [19]. More recently, CPZ (as well as 16 other compounds) has been shown to have antiviral activity against  
76 SARS-CoV-2 on monkey Vero E6 cells [20].  
77 In this context, the aim of the current study was to investigate *in vitro* CPZ antiviral activity against SARS-CoV-2  
78 on monkey Vero E6 cells as well as – for the first time – on human alveolar basal epithelial cells.

79

## 80 **Material and methods**

### 81 2.1 Cell culture and virus isolates

82 Vero E6 cells (African green monkey kidney epithelial cells, ATCC, CRL-1586) were maintained in Dulbecco's  
83 modified Eagle's medium (DMEM) containing 10% foetal bovine serum (FBS) and 5 units/mL penicillin and 5  
84 µg/mL streptomycin at 37°C with 5% CO<sub>2</sub>. A549-ACE2 cells (adenocarcinomic human alveolar basal epithelial  
85 cells, transduced to express the human Angiotensin-converting enzyme 2 (ACE2), kind gift of Pr. O. Schwartz,  
86 Institut Pasteur, Paris France) were maintained in DMEM containing 10% FBS, 5 units/mL penicillin and 5  
87 µg/mL streptomycin and 40 µg/mL blasticidin at 37°C with 5% CO<sub>2</sub>.

88 SARS-CoV-2, isolate BetaCoV/France/IDF0372/2020 C2, was supplied by the National Reference Centre for  
89 Respiratory Viruses (NRC) hosted at Institut Pasteur (Paris, France) and headed by Pr. S. Van der Werf. The  
90 human sample from which this strain was isolated has been provided by Dr. X. Lescure and Pr. Y. Yazdanpanah  
91 from the Bichat Hospital, Paris, France. Viral stocks were prepared by propagation in VeroE6 cells in DMEM  
92 supplemented with 2% FBS. Viral titres were determined by plaque assay. All experiments involving live SARS-  
93 CoV-2 were performed in compliance with Institut Pasteur guidelines for Biosafety Level 3 work. All  
94 experiments were performed in at least three biologically independent replicates.

95

### 96 2.2 Antiviral activity assay

97 Cells were seeded into 96-well plates 24 h prior to the experiment. Two hours prior to infection, cell culture  
98 supernatant was replaced with media containing 32µM, 16µM, 8µM, 4µM and 2µM of CPZ, or the equivalent  
99 volume of maximum H<sub>2</sub>O vehicle used as a control. For the infection, the drug-containing media was removed,  
100 and replaced with virus inoculum (MOI of 0.1 PFU/cell for VeroE6 and 1 for A549-ACE2) for 2 hours. The  
101 inoculum was then removed and replaced with 100µl fresh media (2% FBS) containing CPZ at the indicated  
102 concentrations or H<sub>2</sub>O and incubated for 48 hours.

103 At 48h, cell supernatant was collected and spun for 5 min at 3,000g to remove debris. Toxicity controls were  
104 setup in parallel on uninfected cells. RNA was extracted from 50µl aliquots of supernatant using the  
105 Nucleospin 96 virus kit (Macherey-Nagel) following the manufacturer's instructions. Detection of viral  
106 genomes was performed by RT-qPCR, using the IP4 primer set developed by the NRC at Institut Pasteur  
107 (described on the WHO website ([https://www.who.int/docs/default-source/coronaviruse/real-time-rt-pcr-](https://www.who.int/docs/default-source/coronaviruse/real-time-rt-pcr-assays-for-the-detection-of-sars-cov-2-institut-pasteur-paris.pdf?sfvrsn=3662fcb6_2)  
108 [assays-for-the-detection-of-sars-cov-2-institut-pasteur-paris.pdf?sfvrsn=3662fcb6\\_2](https://www.who.int/docs/default-source/coronaviruse/real-time-rt-pcr-assays-for-the-detection-of-sars-cov-2-institut-pasteur-paris.pdf?sfvrsn=3662fcb6_2)). RT-qPCR was performed

109 using the Luna Universal One-Step RT-qPCR Kit (NEB) in an Applied Biosystems QuantStudio 3 thermocycler,  
110 using the following cycling conditions: 55°C for 10 min, 95°C for 1 min, and 40 cycles of 95°C for 10 sec,  
111 followed by 60°C for 1 min. The quantity of viral genomes is expressed as PFU equivalents, and was calculated  
112 by performing a standard curve with RNA derived from a viral stock with a known viral titre.  
113 Cell viability in drug-treated cells was measured using the AlamarBlue reagent (ThermoFisher). At 48 h post  
114 treatment, the drug-containing media was removed and replaced with AlamarBlue and incubated for 2h at  
115 37°C. Fluorescence was measured in a Tecan Infinity 2000 plate reader.  
116 Using the same experimental setting, we tested the antiviral activity of remdesivir, as a comparator and a  
117 validator of the experiment.

118

### 119 2.3 Data analysis

120 Antiviral activity was assayed as a percentage of inhibition of SARS-CoV-2, normalized to the quantity of viral  
121 genomes under the lowest concentration of CPZ (i.e. 2 µM) for each of the three independent replicates.  
122 Percentage cytotoxicity was calculated relative to untreated cells (0% toxicity). Antiviral activity and cytotoxicity  
123 data were analysed using GraphPad Prism version 8.4.2 for MacOS (GraphPad Software, San Diego, California  
124 USA, [www.graphpad.com](http://www.graphpad.com)). Non-linear regressions were performed and IC50 (half maximal inhibitory  
125 concentration), IC90 (90% maximal inhibitory concentration), CC50 (half maximal cytotoxic concentration) and  
126 SI (selectivity index, calculated by dividing the CC50 by the IC50) were calculated from “[Agonist] vs. response -  
127 - Variable slope” curves with constraints to remain above 0% and below 100%.

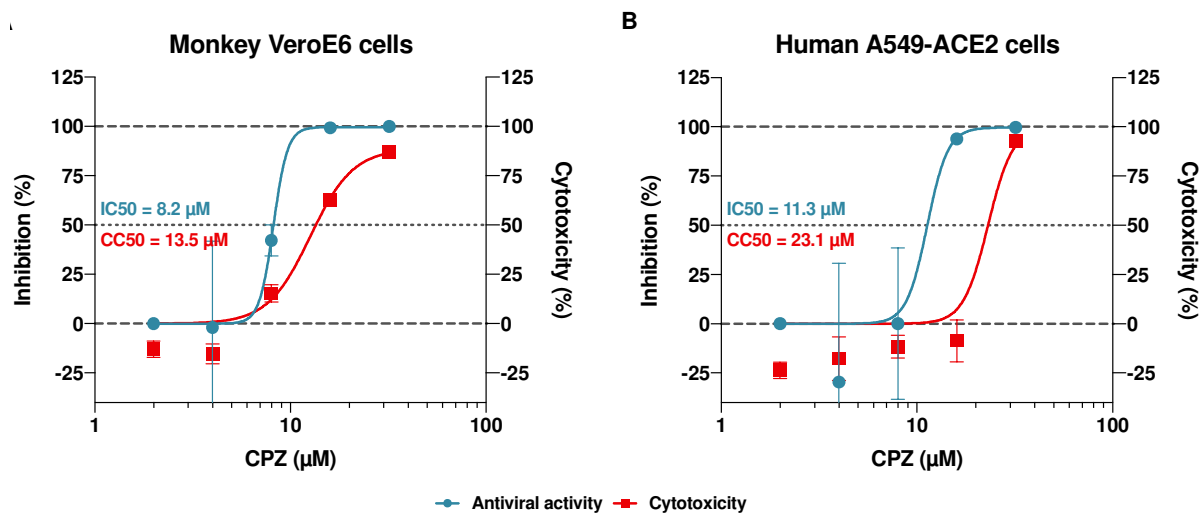
128

## 129 **Results**

130 African Green Monkey VeroE6 cells and human alveolar basal epithelial A549-ACE2 cells were infected with  
131 SARS-CoV-2 in presence of different concentrations of CPZ. Supernatants were harvested at day 2 and  
132 analysed by RT-qPCR for the presence of SARS-CoV-2 RNA. In parallel, cell viability was assessed on non-  
133 infected cells.

134 In monkey VeroE6 cells, we measured an antiviral activity of CPZ against SARS-CoV-2, with an IC50 of 8.2 µM,  
135 an IC90 of 15.2 µM, a CC50 of 13.5µM and thus a SI of 1.65 (Figure 1.A).

136 In human A549-ACE2 cells, CPZ was also associated with an anti-SARS-CoV-2 activity, with an IC<sub>50</sub> of 11.3 μM  
 137 (Figure 1.B) and an IC<sub>90</sub> of 14.3 μM. CPZ was associated with a cytotoxic effect in this model at the highest  
 138 doses assessed, with a CC<sub>50</sub> of 23.1 μM and therefore a SI of 2.04 (Figure 1.B).  
 139 Remdesivir was associated with an antiviral activity against SARS-CoV-2, with an IC<sub>50</sub> of 5 μM in monkey  
 140 VeroE6 cells, and an IC<sub>50</sub> of 0.15 μM in human A549-ACE2 cells.  
 141



142  
 143 **Figure 1.** Antiviral activity of CPZ against SARS-CoV-2 *in vitro* in monkey VeroE6 cells (A) and human A549-ACE2  
 144 cells (B). Viral load in supernatants were measured at 48h (left Y axis), and viability under increasing  
 145 concentrations of the antiviral compound are shown. Error bars denote s.e.m.

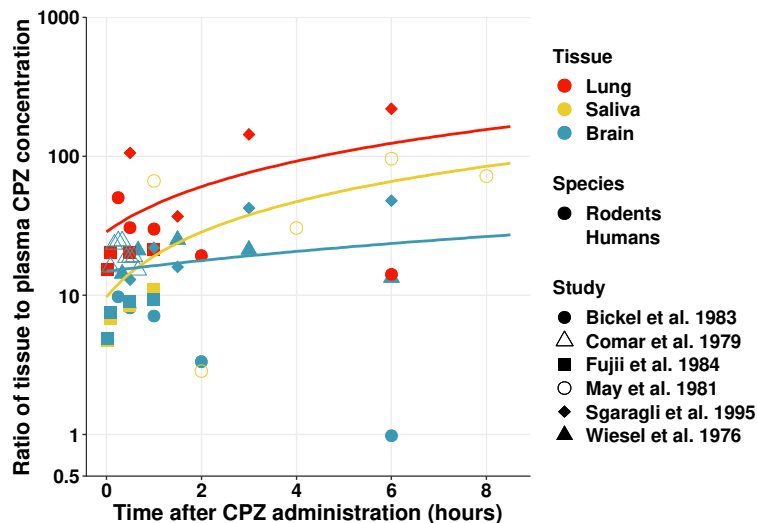
146  
 147 **Discussion**

148 With more than 6 000 000 infections and 370 000 deaths worldwide in just a few months [21], tools are  
 149 urgently needed to help against the SARS-CoV-2 pandemic, to diminish disease severity along with  
 150 contagiousness and to reduce the socio-economic consequences of the pandemic. In this study, we evidenced  
 151 *in vitro* antiviral activity of CPZ against a SARS-CoV-2 isolate in monkey and human cells, with IC<sub>50</sub> of  
 152 respectively 8.2 and 11.3 μM. These results are in line with previous demonstrations of antiviral properties of  
 153 CPZ, a well-known inhibitor of clathrin-mediated endocytosis [11–14], against older coronaviruses. Besides,  
 154 the measured IC<sub>50</sub> of remdesivir are consistent with previously published work [22,23], reinforcing the  
 155 validation of our experimental setup.

156 Even though the measured SI of CPZ are very low, such IC50 measured *in vitro* may translate to CPZ dosage  
157 used in clinical routine. Indeed, one of the main advantages of using CPZ against SARS-CoV-2 could lie in its  
158 biodistribution (Figure 2), and mainly and foremost in its pneumophilic properties. In 1968, Forrest et al.  
159 quantified the CPZ distribution in selected organs through a post-mortem study of 6 patients with  
160 schizophrenia and treated by CPZ until their death [24]. Among the 5 patients with available lung  
161 measurements, the highest CPZ concentration was found in the lungs. These high pneumophilic properties of  
162 CPZ have also been described in preclinical studies, reporting CPZ concentration in the lungs 20 to 200 times  
163 higher than in plasma after a single dose of CPZ [24–27]. Besides the lungs, CPZ concentrations have been  
164 demonstrated to be very high in the salivary glands, 30-100 times higher than in plasma after a single dose of  
165 CPZ [26,28]. In humans, May et al. studied saliva concentration of CPZ in 48 newly admitted patients with  
166 schizophrenia, and saliva concentrations were found to be between 1300 to 22000 ng/ml (*i.e.* 4.1 to 69  $\mu$ M;  
167 CPZ molar mass = 318.86 g/mol) 1 to 8 hours after a single dose of CPZ [28]. These high saliva concentrations  
168 of CPZ could reduce the contagiousness of COVID-19 [29]. Moreover, because of its lipophilic nature, CPZ cross  
169 the blood-brain barrier [30]. CPZ brain distribution, underlying its antipsychotic action and side effects, has  
170 been described with brain to plasma concentration ratio of up to 50 in rodents [25–27,31]. In humans, CPZ  
171 distribution in the brain was studied in 22 patients with schizophrenia in our hospital in 1979, with brain to  
172 plasma ratio ranging from 15 to 25 [32]. This could be of great interest for treating or preventing the  
173 neurological and psychiatric forms of COVID-19 [33] with, to date, no available therapeutic options. Indeed,  
174 remdesivir, anti-IL6 drug tocilizumab and hydroxychloroquine, three of the most studied drugs in the  
175 treatment of COVID-19, do not cross, or cross to a far lesser extent the blood-brain barrier [34–37].

176





177

178 *Figure 2. Review of temporal CPZ biodistribution in lung, saliva and brain. Ratio of tissue to plasma CPZ*  
 179 *concentrations (log scale) after administration of a single dose of CPZ are represented for lung (red), saliva or*  
 180 *salivary glands (yellow) and brain (blue) in rodents (filled) and humans (no-filled). Derived from previous*  
 181 *preclinical and clinical studies [25–28,31,32].*

182

183 Overall, even though the extrapolation from *in vitro* to clinically relevant dosage is not straightforward, the  
 184 IC50 of 11.3  $\mu\text{M}$  (*i.e.* 3603 ng/ml) measured *in vitro* in human cells may be compatible with CPZ dosage used in  
 185 clinical routine. Indeed, residual plasma levels of CPZ in patients range from 30 to 300 ng/ml [38], which could  
 186 correspond to 600 - 60 000 ng/ml in lungs [24–27] and 900 – 30 000 ng/ml in saliva [26,28] according to our  
 187 review (Figure 2). This extrapolation is supported by our observation of lower prevalence of symptomatic and  
 188 severe forms of COVID-19 infections in psychiatric patients.

189 Repurposing CPZ, a molecule already used in clinical practice, could offer both ready-to-use treatment with  
 190 well-known and very mild side effects. CPZ has been widely used in clinical routine in the treatment of acute  
 191 and chronic psychoses for decades. This first antipsychotic medication was discovered in 1952 by Jean Delay  
 192 and Pierre Deniker at Sainte Anne hospital [39]. At this time, CPZ is prescribed for around 70 years and FDA-  
 193 approved in psychiatry and anaesthesiology, with an excellent tolerance profile. CPZ is also used in refractory  
 194 nausea and vomiting of pregnancy [40], in advanced cancer [41], and to treat refractory headaches in various  
 195 neurological conditions [42].

196

197 **Conclusions**

198 This first *in vitro* study of CPZ antiviral activity against SARS-CoV-2 in monkey and human cells supports that  
199 CPZ, a well-known drug with antiviral properties and an excellent tolerance profile, could be tested clinically as  
200 an alternative to currently used drugs or combinations of drugs in COVID-19 treatment. This proof of principle  
201 for the feasibility of CPZ as anti-SARS-CoV-2 therapeutic is a critical step for future clinical trial (NCT04366739).

202

203 **Acknowledgments**

204 We are grateful to the Centre National de Reference des virus des infections respiratoires for sharing reagents  
205 and protocols. We thank Olivier Schwartz and his team for sharing the A549-ACE2 cell line. The authors wish to  
206 thank the Fondation Pierre Deniker for its support.

207

208

209 **Author contributions**

210 R.G., F.C., E.S.L and M.P. designed the study. E.S.L., M.Pr., L.L. and J.C. performed the experiments. E.S.L.,  
211 M.Pr., L.L, M.P., A.C. and D.A. analyzed the data. R.G., E.S.L., A.C., M.P. and D.A. wrote the paper with input  
212 from F.C., G.F., A.-C.P., M.B., F.V. and F.P.-D. All authors have approved the final article.

213

214 **Declarations**

215 **Funding:** This study has received funding from Institut Pasteur (covid-therap), the French Government's  
216 Investissement d'Avenir program, Laboratoire d'Excellence "Integrative Biology of Emerging Infectious  
217 Diseases" (grant n°ANR-10-LABX-62-IBEID). ESL acknowledges funding from the INCEPTION program  
218 (Investissements d'Avenir grant ANR-16-CONV-0005).

219 **Competing Interests:** No conflict of interest

220 **Ethical Approval:** Not required

221

222 **References**

- 223 [1] Plaze M, Attali D, Petit A-C, Blatzer M, Simon-Loriere E, Vinckier F, et al. Repositionnement de la  
224 chlorpromazine dans le traitement du COVID-19: étude reCoVery. *L'Encéphale* 2020.  
225 <https://doi.org/10.1016/j.encep.2020.04.010>.
- 226 [2] Krizanová O, Ciampor F, Veber P. Influence of chlorpromazine on the replication of influenza virus in chick  
227 embryo cells. *Acta Virol* 1982;26:209–16.
- 228 [3] Blanchard E, Belouzard S, Goueslain L, Wakita T, Dubuisson J, Wychowski C, et al. Hepatitis C virus entry  
229 depends on clathrin-mediated endocytosis. *J Virol* 2006;80:6964–72. [https://doi.org/10.1128/JVI.00024-](https://doi.org/10.1128/JVI.00024-06)  
230 06.
- 231 [4] Pohjala L, Utt A, Varjak M, Lulla A, Merits A, Ahola T, et al. Inhibitors of Alphavirus Entry and Replication  
232 Identified with a Stable Chikungunya Replicon Cell Line and Virus-Based Assays. *PLOS ONE*  
233 2011;6:e28923. <https://doi.org/10.1371/journal.pone.0028923>.
- 234 [5] Pho MT, Ashok A, Atwood WJ. JC virus enters human glial cells by clathrin-dependent receptor-mediated  
235 endocytosis. *J Virol* 2000;74:2288–92. <https://doi.org/10.1128/jvi.74.5.2288-2292.2000>.
- 236 [6] Nawa M, Takasaki T, Yamada K-I, Kurane I, Akatsuka T. Interference in Japanese encephalitis virus  
237 infection of Vero cells by a cationic amphiphilic drug, chlorpromazine. *J Gen Virol* 2003;84:1737–41.  
238 <https://doi.org/10.1099/vir.0.18883-0>.
- 239 [7] Chu VC, McElroy LJ, Ferguson AD, Bauman BE, Whittaker GR. Avian infectious bronchitis virus enters cells  
240 via the endocytic pathway. *Adv Exp Med Biol* 2006;581:309–12. [https://doi.org/10.1007/978-0-387-](https://doi.org/10.1007/978-0-387-33012-9_54)  
241 33012-9\_54.
- 242 [8] Pu Y, Zhang X. Mouse Hepatitis Virus Type 2 Enters Cells through a Clathrin-Mediated Endocytic Pathway  
243 Independent of Eps15. *Journal of Virology* 2008;82:8112–23. <https://doi.org/10.1128/JVI.00837-08>.
- 244 [9] Persaud M, Martinez-Lopez A, Buffone C, Porcelli SA, Diaz-Griffero F. Infection by Zika viruses requires the  
245 transmembrane protein AXL, endocytosis and low pH. *Virology* 2018;518:301–12.  
246 <https://doi.org/10.1016/j.virol.2018.03.009>.
- 247 [10] Carro AC, Piccini LE, Damonte EB. Blockade of dengue virus entry into myeloid cells by endocytic inhibitors  
248 in the presence or absence of antibodies. *PLoS Negl Trop Dis* 2018;12:e0006685.  
249 <https://doi.org/10.1371/journal.pntd.0006685>.
- 250 [11] Daniel JA, Chau N, Abdel-Hamid MK, Hu L, von Kleist L, Whiting A, et al. Phenothiazine-derived  
251 antipsychotic drugs inhibit dynamin and clathrin-mediated endocytosis. *Traffic* 2015;16:635–54.  
252 <https://doi.org/10.1111/tra.12272>.

- 253 [12] Wang LH, Rothberg KG, Anderson RG. Mis-assembly of clathrin lattices on endosomes reveals a regulatory  
254 switch for coated pit formation. *J Cell Biol* 1993;123:1107–17. <https://doi.org/10.1083/jcb.123.5.1107>.
- 255 [13] Chen F, Zhu L, Zhang Y, Kumar D, Cao G, Hu X, et al. Clathrin-mediated endocytosis is a candidate entry  
256 sorting mechanism for *Bombyx mori* cypovirus. *Sci Rep* 2018;8:7268. [https://doi.org/10.1038/s41598-](https://doi.org/10.1038/s41598-018-25677-1)  
257 018-25677-1.
- 258 [14] Inoue Y, Tanaka N, Tanaka Y, Inoue S, Morita K, Zhuang M, et al. Clathrin-dependent entry of severe acute  
259 respiratory syndrome coronavirus into target cells expressing ACE2 with the cytoplasmic tail deleted. *J*  
260 *Viro* 2007;81:8722–9. <https://doi.org/10.1128/JVI.00253-07>.
- 261 [15] Burkard C, Verheije MH, Wicht O, Kasteren SI van, Kuppeveld FJ van, Haagmans BL, et al. Coronavirus Cell  
262 Entry Occurs through the Endo-/Lysosomal Pathway in a Proteolysis-Dependent Manner. *PLOS*  
263 *Pathogens* 2014;10:e1004502. <https://doi.org/10.1371/journal.ppat.1004502>.
- 264 [16] Yang N, Shen H-M. Targeting the Endocytic Pathway and Autophagy Process as a Novel Therapeutic  
265 Strategy in COVID-19. *Int J Biol Sci* 2020;16:1724–31. <https://doi.org/10.7150/ijbs.45498>.
- 266 [17] de Wilde AH, Jochmans D, Posthuma CC, Zevenhoven-Dobbe JC, van Nieuwkoop S, Bestebroer TM, et al.  
267 Screening of an FDA-approved compound library identifies four small-molecule inhibitors of Middle East  
268 respiratory syndrome coronavirus replication in cell culture. *Antimicrob Agents Chemother*  
269 2014;58:4875–84. <https://doi.org/10.1128/AAC.03011-14>.
- 270 [18] Dyal J, Coleman CM, Hart BJ, Venkataraman T, Holbrook MR, Kindrachuk J, et al. Repurposing of clinically  
271 developed drugs for treatment of Middle East respiratory syndrome coronavirus infection. *Antimicrob*  
272 *Agents Chemother* 2014;58:4885–93. <https://doi.org/10.1128/AAC.03036-14>.
- 273 [19] Cong Y, Hart BJ, Gross R, Zhou H, Frieman M, Bollinger L, et al. MERS-CoV pathogenesis and antiviral  
274 efficacy of licensed drugs in human monocyte-derived antigen-presenting cells. *PLOS ONE*  
275 2018;13:e0194868. <https://doi.org/10.1371/journal.pone.0194868>.
- 276 [20] Weston S, Coleman CM, Haupt R, Logue J, Matthews K, Li Y, et al. Broad anti-coronaviral activity of FDA  
277 approved drugs against SARS-CoV-2 in vitro and SARS-CoV in vivo. *Journal of Virology* 2020.  
278 <https://doi.org/10.1128/JVI.01218-20>.
- 279 [21] COVID-19 situation update worldwide, as of 1 June 2020. European Centre for Disease Prevention and  
280 Control n.d. <https://www.ecdc.europa.eu/en/geographical-distribution-2019-ncov-cases> (accessed June  
281 1, 2020).
- 282 [22] Wang M, Cao R, Zhang L, Yang X, Liu J, Xu M, et al. Remdesivir and chloroquine effectively inhibit the  
283 recently emerged novel coronavirus (2019-nCoV) in vitro. *Cell Research* 2020;30:269–71.  
284 <https://doi.org/10.1038/s41422-020-0282-0>.
- 285 [23] Jeon S, Ko M, Lee J, Choi I, Byun SY, Park S, et al. Identification of Antiviral Drug Candidates against SARS-  
286 CoV-2 from FDA-Approved Drugs. *Antimicrobial Agents and Chemotherapy* 2020;64.  
287 <https://doi.org/10.1128/AAC.00819-20>.
- 288 [24] Forrest IS, Bolt AG, Serra MT. Distribution of chlorpromazine metabolites in selected organs of psychiatric  
289 patients chronically dosed up to the time of death. *Biochem Pharmacol* 1968;17:2061–70.  
290 [https://doi.org/10.1016/0006-2952\(68\)90180-9](https://doi.org/10.1016/0006-2952(68)90180-9).
- 291 [25] Bickel MH, Graber BE, Moor M. Distribution of chlorpromazine and imipramine in adipose and other  
292 tissues of rats. *Life Sci* 1983;33:2025–31. [https://doi.org/10.1016/0024-3205\(83\)90742-7](https://doi.org/10.1016/0024-3205(83)90742-7).
- 293 [26] Fujii T, Miyazaki H, Nambu K, Matsumoto K, Hashimoto M. Autoradiographic and biochemical studies of  
294 drug distribution in the liver. II. [<sup>35</sup>S]Chlorpromazine and [<sup>14</sup>C]imipramine. *Eur J Drug Metab*  
295 *Pharmacokinet* 1984;9:247–55. <https://doi.org/10.1007/BF03189648>.
- 296 [27] Sgaragli GP, Valoti M, Palmi M, Frosini M, Giovannini MG, Bianchi L, et al. Rat tissue concentrations of  
297 chlorimipramine, chlorpromazine and their N-demethylated metabolites after a single oral dose of the  
298 parent compounds. *J Pharm Pharmacol* 1995;47:782–90. [https://doi.org/10.1111/j.2042-](https://doi.org/10.1111/j.2042-7158.1995.tb06741.x)  
299 7158.1995.tb06741.x.
- 300 [28] May PR, Van Putten T, Jenden DJ, Yale C, Dixon WJ. Chlorpromazine levels and the outcome of treatment  
301 in schizophrenic patients. *Arch Gen Psychiatry* 1981;38:202–7.  
302 <https://doi.org/10.1001/archpsyc.1981.01780270088012>.
- 303 [29] To KK-W, Tsang OT-Y, Leung W-S, Tam AR, Wu T-C, Lung DC, et al. Temporal profiles of viral load in  
304 posterior oropharyngeal saliva samples and serum antibody responses during infection by SARS-CoV-2:  
305 an observational cohort study. *Lancet Infect Dis* 2020. [https://doi.org/10.1016/S1473-3099\(20\)30196-1](https://doi.org/10.1016/S1473-3099(20)30196-1).
- 306 [30] Rundle-Thiele D, Head R, Cosgrove L, Martin JH. Repurposing some older drugs that cross the blood–brain  
307 barrier and have potential anticancer activity to provide new treatment options for glioblastoma. *Br J*  
308 *Clin Pharmacol* 2016;81:199–209. <https://doi.org/10.1111/bcp.12785>.

- 309 [31] Wiesel FA, Alfredsson G. The distribution and metabolism of chlorpromazine in rats and the relationship  
310 to effects on cerebral monoamine metabolism. *Eur J Pharmacol* 1976;40:263–72.  
311 [https://doi.org/10.1016/0014-2999\(76\)90061-3](https://doi.org/10.1016/0014-2999(76)90061-3).
- 312 [32] Comar D, Zarifian E, Verhas M, Soussaline F, Maziere M, Berger G, et al. Brain distribution and kinetics of  
313 11C-chlorpromazine in schizophrenics: positron emission tomography studies. *Psychiatry Res* 1979;1:23–  
314 9. [https://doi.org/10.1016/0165-1781\(79\)90024-6](https://doi.org/10.1016/0165-1781(79)90024-6).
- 315 [33] Rogers JP, Chesney E, Oliver D, Pollak TA, McGuire P, Fusar-Poli P, et al. Psychiatric and neuropsychiatric  
316 presentations associated with severe coronavirus infections: a systematic review and meta-analysis with  
317 comparison to the COVID-19 pandemic. *The Lancet Psychiatry* 2020;0. [https://doi.org/10.1016/S2215-0366\(20\)30203-0](https://doi.org/10.1016/S2215-0366(20)30203-0).
- 319 [34] Warren TK, Jordan R, Lo MK, Ray AS, Mackman RL, Soloveva V, et al. Therapeutic efficacy of the small  
320 molecule GS-5734 against Ebola virus in rhesus monkeys. *Nature* 2016;531:381–5.  
321 <https://doi.org/10.1038/nature17180>.
- 322 [35] Acharya UH, Dhawale T, Yun S, Jacobson CA, Chavez JC, Ramos JD, et al. Management of cytokine release  
323 syndrome and neurotoxicity in chimeric antigen receptor (CAR) T cell therapy. *Expert Rev Hematol*  
324 2019;12:195–205. <https://doi.org/10.1080/17474086.2019.1585238>.
- 325 [36] Hunter BD, Jacobson CA. CAR T-cell associated neurotoxicity: Mechanisms, clinicopathologic correlates,  
326 and future directions. *J Natl Cancer Inst* 2019. <https://doi.org/10.1093/jnci/djz017>.
- 327 [37] Richardson PJ, Ottaviani S, Prella A, Stebbing J, Casalini G, Corbellino M. CNS penetration of potential anti-  
328 COVID-19 drugs. *J Neurol* 2020:1–3. <https://doi.org/10.1007/s00415-020-09866-5>.
- 329 [38] Hiemke C, Bergemann N, Clement HW, Conca A, Deckert J, Domschke K, et al. Consensus Guidelines for  
330 Therapeutic Drug Monitoring in Neuropsychopharmacology: Update 2017. *Pharmacopsychiatry*  
331 2018;51:9–62. <https://doi.org/10.1055/s-0043-116492>.
- 332 [39] Delay J, Deniker P, Harl JM. [Therapeutic use in psychiatry of phenothiazine of central elective action  
333 (4560 RP)]. *Ann Med Psychol (Paris)* 1952;110:112–7.
- 334 [40] Committee on Practice Bulletins-Obstetrics. ACOG Practice Bulletin No. 189: Nausea And Vomiting Of  
335 Pregnancy. *Obstet Gynecol* 2018;131:e15–30. <https://doi.org/10.1097/AOG.0000000000002456>.
- 336 [41] Gupta M, Davis M, Walsh D, LeGrand S, Lagman R, Parala-Metz A. Nausea and Vomiting in Advanced  
337 Cancer—The Cleveland Clinic Protocol (TH310). *Journal of Pain and Symptom Management*  
338 2013;45:338–9. <https://doi.org/10.1016/j.jpainsymman.2012.10.042>.
- 339 [42] Marmura MJ, Silberstein SD, Schwedt TJ. The Acute Treatment of Migraine in Adults: The American  
340 Headache Society Evidence Assessment of Migraine Pharmacotherapies. *Headache: The Journal of Head  
341 and Face Pain* 2015;55:3–20. <https://doi.org/10.1111/head.12499>.
- 342